Vibration Analysis of HDD Actuator with Equivalent Finite Element Model of VCM Coil

Dong-Woohn Kim
Graduate School, Department of Mechanical Engineering, Yonsei University
Shinchon-dong 134, Sudaemoon-ku, Seoul 120-749, Korea
Jin-Koo Lee
Engineer, MANDO Corporation
No-Cheol Park*
Professor, Center for Information Storage Device (CISD), Yonsei University
Shinchon-dong 134, Sudaemoon-ku, Seoul 120-749, Korea
Young-Pil Park
Professor, Department of Mechanical Engineering, Yonsei University,
Shinchon-dong 134, Sudaemoon-ku, Seoul 120-749, Korea

As the rate of increase in areal density of the HDD has accelerated, dynamic characteristics of the HDD actuator need to be improved with respect to the performance of the tracking servo and shock transmission. Therefore, it is important to analyze the vibration characteristic of the HDD actuator that consists of the VCM part, E-block and pivot bearing. In this paper, vibration modes of the HDD actuator are investigated the using finite element and experimental modal analyses methods. To develop a detailed finite element model, finite element models of each components of the actuator assembly are constructed and tuned to the results of the EMA. The VCM coil is modeled as an equivalent finite element model that has an orthotropic material property using auto-model updating program. Auto-model updating program with improved sensitivity based iterative method is applied to build a detailed finite element model using the result of the EMA. A detailed finite element model of the HDD actuator is then constructed and analyzed.

Key Words: HDD (Hard Disk Drive), Actuator, Dynamic Characteristics, Vibration Mode, Finite Element Model Updating, Sensitivity Analysis, Finite Difference Method

Nomenclature

α	: Weighting factor
E_x, E_y, E_z	: Young's modulus
G_{xy}, G_{xz}, G_{yz}	: Shear elastic modulus
$\nu_{xy}, \nu_{xy}, \nu_{yz}$	: Poission's ratio
λ_i	: Eigen-value
N	: The number of modal parameters
M	: The number of design variables
θ_i	: Modal parameter
ζ_j	: Design variable
$\{\phi\}_i$	: Eigen-vector
$\{\phi_C\}$	: Calculated eigen-vector
$\{\phi_T\}$	: Measured eigen-vector
$\{\theta_T\}$	: Reference modal parameter vector
$\{\theta_C\}$	: Predicted modal parameter vector
$\{\Delta\theta\}$	: Error vector for modal parameters
$\{\zeta_u\}$	: Updated design variable vector
$\{\zeta_o\}$	: Current design variable vector
$\{\Delta\zeta\}$	: Modification vector of design variables
[S]	: Sensitivity matrix

* Corresponding Author,
E-mail : pnch@yonsei.ac.kr
TEL : +82-2-2123-4530; **FAX** : +82-2-365-8460
Professor, Center for Information Storage Device (CISD), Yonsei University Shinchon-dong 134, Sudaemoon-ku, Seoul 120-749, Korea. (Manuscript **Received** September 11, 2002; **Revised** February 3, 2003)

1. Introduction

An important primary trend in hard disk drives is that the areal density and storage capacity are increasing very rapidly. To maintain the areal density growth, the performance of the track following servo must be upgraded. The servo gain is limited by the mechanical resonance of the actuator structure that moves the read/write heads across the data tracks on the disk surfaces and holds them over the specific track for reading and writing information (Heath, 2000).

Hard disk drives (HDDs) contain high performance electro-mechanical components and the actuator structure is one of the major components. Figure 1 shows the schematic of an actuator structure in hard disk drives. The actuator consists of the heads, suspensions, arms of E-block, pivot shaft, ball bearing and the VCM (Voice Coil Motor) part including the VCM coil and VCM holder. A magnetic read/write head is mounted onto the slider that constitutes a part of the suspension. A suspension in the actuator structure connects the sliders to the VCM. The actuator structure also is called the head stack assembly (HSA).

It is known that the slider moves off from the centerline of the HSA in some vibration modes and generates the residual vibration in the track following operation. The suspension sway mode and the quasi-rigid-body mode of the HSA are two important vibration modes that cause the significant off-track error. Since the linear actuator has been replaced by the rotary actuator to achieve high speed and small-sized disk drive, the acceleration in the lateral direction of the suspension assembly during access has become an important problem. Therefore, the bandwidth of the positioning servo is limited by the resonant frequency of the suspension assembly in the direction of the access (Ohwe et al., 1990). Throughout the disk drive industry, it is accepted that in order to ensure adequate system performance, the frequency of the lowest structural resonance must be at least two octaves above the bandwidth of the servo system (Miu et al., 1991; Chiou et al., 1992). To develop high track density disk drives, the dynamic characteristics of the suspension are investigated using the experimental modal analysis and the finite element analysis (Kim C. J. et al., 1997). The sway mode of the suspension is the primary source of radial slider motions (Chiou et al., 1992). Since 1990, size of the slider has decreased due to rapid development of technology such as MR and GMR Head. The frequency of the sway mode has increased to over 8 kHz due to new design of the suspension and pico-slider (Ohwe et al., 1996).

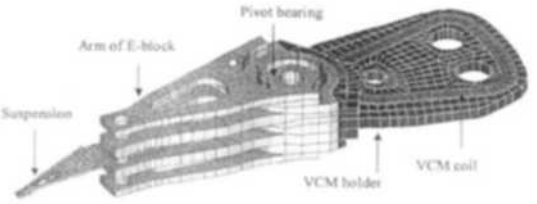

Fig. 1 Schematic of the actuator structure

It is common feature of the present hard disk drives that a QR mode exists in 3~5 kHz range and it is the lowest vibration mode that limits the tracking servo bandwidth. The QR mode involves coupled vibration of the VCM part, arm of E-block and a ball bearing assembly. The system mode, which is generated by the distortion of the ball bearing, is particularly troublesome for the servo system since it is very sensitive to the assembly process (Jiang L. et al., 1999).

Recently, the shock resistance of hard disk drives has become an important issue for mobile computers and portable electronics. The head slap motion of the slider triggered by a shock load causes the collision with the disk surface. In this phenomenon, the read/write error and permanent damage may occur (Steve Marek et al., 1995). To understand the shock mechanism of the HDD actuator, the shock transmissibility of the actuator structure and the beating between the arm blade of E-block and the suspension are investigated (Jin-Seung Sohn et al. 2001). It is found that the first bending mode of the arm blade plays an important role in the shock transmissibility.

Proper understanding of the dynamic properties of the actuator is essential for the new drive

design and redesign of the actuator system. In this paper, we investigate the dynamic characteristics of the actuator in detail by employing both the experimental and numerical methods. To develop an accurate finite element model of this complex structure, finite element models of subcomponents are constructed and then combined to form an assembly model of the actuator. In the case of the VCM coil, an equivalent finite element model of the coil bundle is developed using the result of the experimental modal analysis. Numerous works on the finite element model updating using measurement are available. Sensitivity based iterative finite element model updating process is an effective method to apply to an actual mechanical component (Kukil Sohn et al. 1992). When the finite element model updating for the complex structure is performed using this method, some limitation must be considered. Firstly, proper selection of the design variables and the initial values of modal parameters are important to achieve the numerical convergence of the results. Next, the variation of the design variables must be kept to within bounds to maintain physical meaning. In this research, the sensitivity matrix of the modal parameters with respect to the material properties is calculated using a finite difference method and the least squares parameter estimation is performed with improved strategy for selection of the design variables. A commercial CAE software, MATLAB and ANSYS are used to construct the auto-model updating program.

2. Equivalent Finite Element Model for VCM Coil

2.1 Finite element model updating using an iterative modal sensitivity approach

The correction of the analytical model is a main step of the updating procedure. Many correction procedures have been presented and categorized into two main groups, direct methods and sensitivity based iterative methods. The direct methods calculate updated system matrices in one sigle step and all elements of the system matrices are variable. The direct method with iterative calculation of the sensitivity coefficient also has weak points in that the mass and stiffness matrices are design parameters and this method is hard to apply to finite element models with physical design parameters such as the material porperties (Lee J. Y., 2002).

Sensitivity based methods optimize selected updating parameters in an iterative procedure based on truncated Taylor's expansions that express the modal parameters, the system matrices and related characteristics as a function of the updating parameters. The method of finite element model updating using an iterative modal sensitivity approach corrects the design variables such as the material properties, the thickness of the plate, the joint stiffness, etc. It is called the sensitivity-based design parameter method because the physical parameters defined as the design variables are updated from the result of the sensitivity analysis (Sun et al., 2000). A modal sensitivity coefficient is defined as the rates of change of the modal parameter θ_i with respect to the design variable ζ_j, computed at a given state of the design variabls. When the differential is computed for all selected modal parameters with respect to all selected design variables, the sensitivity matrix $[S]$ is obtained :

$$[S]=S_{ij}=\left[\frac{\partial\theta_i}{\partial\zeta_j}\right] \tag{1}$$

where, $i=1, \cdots, N$; Modal parameters
$j=1, \cdots, M$; Design variables

The objective of any model updating is to adjust the values of selected design variables such that a reference correlation coefficient is minimized. The functional relationship between the modal parameters and the design variables can be expressed in terms of a Taylor series expansion limited to the linear term.

$$\{\theta_T\}=\{\theta_C\}+[S](\{\zeta_u\}-\{\zeta_o\}) \tag{2}$$

$$\{\Delta\theta\}=[S]\{\Delta\zeta\} \tag{3}$$

where, $\{\theta_T\}$: Reference modal parameter vector (measure)
$\{\theta_C\}$: Predicted modal parameter vector for a given state $\{\zeta_o\}$ of the design variables.
$\{\zeta_u\}$: Updated design variable vector

$[S]$: Sensitivity matrix

For a precise finite element model of the structure, model-updating process is performed as follows :

(1) Construct the modal parameter vector θ.

$$\{\theta\}=[\theta_1, \theta_2, \cdots, \theta_N]^T \quad (4)$$

The error vector is represented by

$$\{\Delta\theta\}=\{\theta_T\}-\{\theta_C\}, \quad (5)$$

where the measured modal parameter vector θ_T is a reference vector, and θ_C is a predicted modal parameter vector with current design variables.

(2) Determine the design variables ζ_j(j=1, 2, ⋯, M) for structural modification.

Modification vector $\{\Delta\zeta\}$ is defined as

$$\{\Delta\zeta\}=[\Delta\zeta_1, \Delta\zeta_2, \cdots, \Delta\zeta_M]^T \quad (6)$$

(3) Calculate a sensitivity matrix $[S]$ using the finite difference method. The first order sensitivity matrix of the modal parameters for the design variables is written as

$$[S]=\begin{bmatrix} \frac{\Delta\theta_1}{\Delta\zeta_1} & \frac{\Delta\theta_1}{\Delta\zeta_2} & \cdots, & \frac{\Delta\theta_1}{\Delta\zeta_M} \\ \frac{\Delta\theta_2}{\Delta\zeta_1} & \frac{\Delta\theta_2}{\Delta\zeta_2} & \cdots, & \frac{\Delta\theta_2}{\Delta\zeta_M} \\ \cdots & \cdots & \cdots, & \cdots \\ \frac{\Delta\theta_N}{\Delta\zeta_1} & \frac{\Delta\theta_N}{\Delta\zeta_2} & \cdots, & \frac{\Delta\theta_N}{\Delta\zeta_M} \end{bmatrix} \quad (7)$$

Hence, the variation in the modal parameter due to the structural modification is expressed as

$$\{\Delta\theta\}=[S]\{\Delta\zeta\} \quad (8)$$

(4) Desired variation vector of the design variables can be obtained as follows :

$$\{\Delta\zeta\}=[S]^{-1}\{\Delta\theta\}, \; N=M \quad (9)$$

If each selected design variable is independent and the rank of the sensitivity matrix $[S]$ is equal to the number M, the inverse of the sensitivity matrix $[S]^{-1}$ exists. Generally, the number of the modal parameter N is not equal to the number of the design variable M. If N is not equal to M, the pseudo inverse matrix method is used as follows :

$$\{\Delta\zeta\}=[S]^T([S][S]^T)^{-1}\{\Delta\theta\}, \; N<M \quad (10)$$

$$\{\Delta\zeta\}=([S]^T[S])^{-1}[S]^T\{\Delta\theta\}, \; N>M \quad (11)$$

(5) Update the design variable vector and iterate the finite element steps analysis until the convergence criteria are satisfied.

$$\{\zeta\}^{i+1}=\{\zeta\}^i+\alpha\{\Delta\zeta\} \quad (12)$$

The sensitivity matrix $[S]$ is constructed using only the first order sensitivity. Hence, the weighting factor α is employed to prevent the divergence.

Fig. 2 shows the flow chart of an auto-model updating program. The eigen value λ_i and eigen vector $\{\phi\}_i$ are calculated by the finite element analysis and compared with the results of the modal testing. The modal assurance criterion (MAC) numerically compares all mode shapes of the finite element analysis with all mode shapes of the EMA to identify the calculated modes (Ward Heylen et al., 1997). The following equation is

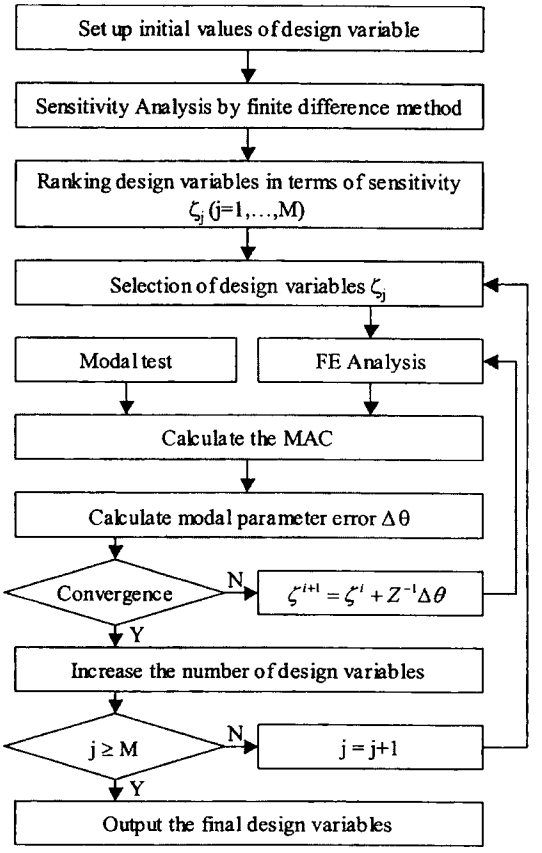

Fig. 2 The flow chart of auto-model updating program

used :

$$MAC(\phi_C, \phi_T) = \frac{|\{\phi_C\}^T\{\phi_T\}|^2}{(\{\phi_C\}^T\{\phi_C\})(\{\phi_T\}^T\{\phi_T\})} \quad (13)$$

where, $\{\phi_C\}$: eigen vector calculated by finite element analysis

$\{\phi_T\}$: eigen vector estimated by EMA

Design variables for the finite element model updating are selected and the sensitivities of the modal parameters are calculated to arrange the design variables in ascending order. The sensitivity matrix is calculated using the finite difference method and modified values of the design variables are estimated by the inverse matrix method given by Eq. (9). As a result of the inversion of the sensitivity matrix, calculated variation of the design variables with larger sensitivity is smaller than that with smaller sensitivity. It is clear that the variation rate of a less sensitive updating parameter must larger than that of a more sensitive updating parameter in order to generate the same amount of $\Delta\theta$ for correction. This feature of the updating algorithm suppresses the variation ranges of the more sensitive updating parameters and causes the meaninglessly large variations of the less sensitive updating parameters over the linearization range of interest. When the norm of the error of a modal parameter between the reference value and current value is large, desired variation of the design variable with large sensitivity must be increased in order to obtain convergence.

Fig. 2 shows the detailed algorithm of the improved sensitivity based iterative method. This improved sensitivity based iterative method has different characteristics compared with the conventional sensitivity based iterative method as follows :

• Sensitivity of the modal parameter vector with respect to the updating parameters is evaluated using the norm of the sensitivity to rank the updating parameter in terms of sensitivity magnitude. The updating parameters are rearranged in descending order so that the most sensitive updating parameter is arranged in the first position.

• As shown in Fig. 2, the number of selected updating parameters is increased gradually in each outer loop step in which the conventional sensitivity based iterative method is performed. In the first step of the outer loop, the most sensitive updating parameter is only used for model correction to minimize the error norm between the analytical modal parameters and the experimental modal parameters. In the next step of the outer loop, the most and the second-most sensitive updating parameters are used. The greater the iteration number in the outer loop, the greater the number of updating parameters are in descending order.

This improved method can protect the numerical results from divergence and help maintain proper convergence.

2.2 Sensitivity analysis and model updating for the VCM coil

The FRF (frequency response function) of the VCM coil is measured on a soft sponge in both vertical and horizontal directions. The rigid mode due to the soft sponge is sufficiently lower than the first local mode of the VCM coil and hence the boundary condition of the test specimen is considered to be freely supported. As shown in Fig. 4, impulse force is applied to the VCM coil by a small impact hammer (PCB Type 086C80). In Fig. 4, the size of the test specimen and the impact hammer are compared to a coin to emphasize their small dimensions. The velocity response of the VCM coil is measured by the laser doppler vibrometer (Polytec LDV) at 12 points in the vertical direction and 10 points in the horizontal direction. Measured signals of the impulse force and velocity responses are sent to a 4-channel dynamic signal analyzer (HP35670A) to acquire the frequency response function. Fig. 3 shows the experimental setup for the experimental modal analysis of the VCM coil. The measured frequency function is averaged ten times. The modal parameters are estimated using SMS Star-Modal, a modal parameter estimation software. Since the impact hammer cannot readily excite the test specimen for over 15 kHz range, the frequency range for measurement is limited to the range of 0 to 12 kHz. There are 8 vibration modes in this frequency range. Measured natural frequencies and mode shapes are presented in Fig. 5. In Fig.

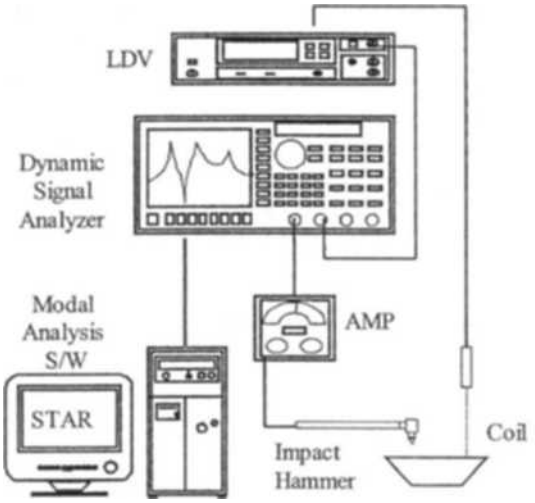

Fig. 3 Experimental setup

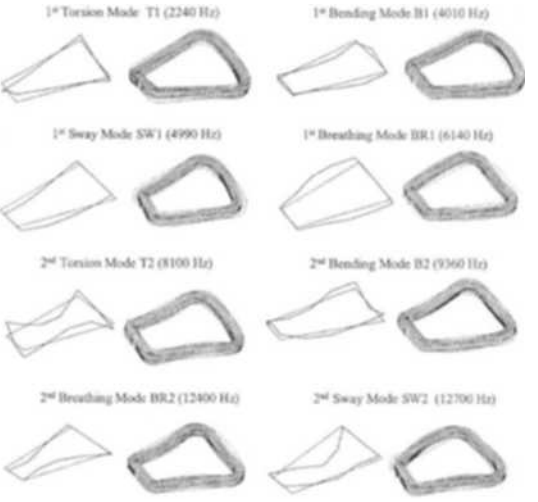

Fig. 5 Measured natural frequencies and mode shapes of VCM coil

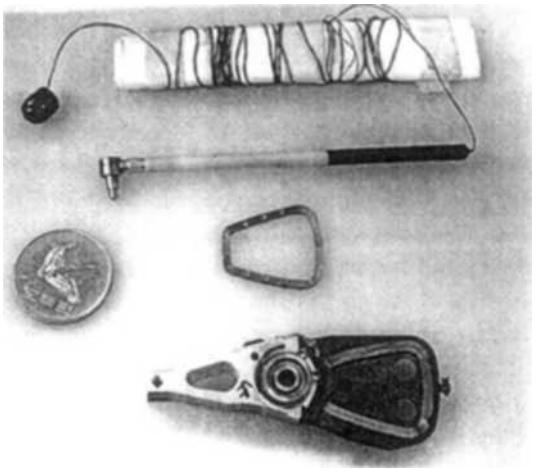

Fig. 4 Test specimen and impact hammer

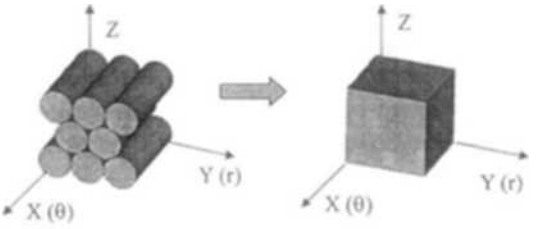

Fig. 6 Modeling of the VCM coil

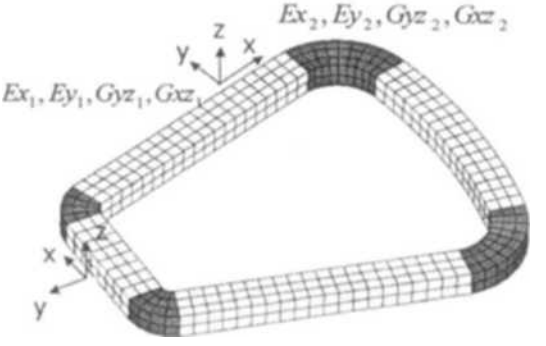

Fig. 7 Design variables of the VCM coil

5, measured mode shapes are compared with calculated mode shapes of the finite element model.

As shown in Fig. 6, the VCM coil is piled on top of the fine coil by applying adhesive. In this study, the VCM coil is modeled as an equivalent finite element model using a solid element with an orthotropic property to properly represent the coil structure. Fig. 7 shows the equivalent finite element model. Five local coordinates are introduced partly in the VCM coil and six parameters are used to idealize the VCM coil as an orthotropic material as follows :

$E_x(E_\theta)$, $E_y(E_r)=E_z(E_z)$, $G_{xy}(G_{r\theta})=G_{xz}(G_{\theta z})$, $G_{yz}(G_{rz})$, $\upsilon_{xy}=\upsilon_{xz}$, υ_{yz}.

The finite element model has different properties at the corner compared with those of linear part to build a proper model. Hence, eight design variables of the VCM coil model are determined as follows :

Table 1 Natural frequencies of initial and updated finite element model

Mode	EMA [Hz]	Initial finite element Model			Updated finite element Model		
		FEA [Hz]	E [%]	MAC	FEA [Hz]	E [%]	MAC
T1	2240	3040	35.8	0.925	2276	1.61	0.934
B1	4010	3730	−7.02	0.881	4182	4.28	0.902
SW1	4990	4520	−9.41	0.980	5059	1.38	0.977
BR1	6140	5360	−12.6	0.929	6296	2.54	0.930
T2	8100	8120	0.24	0.855	7782	−3.92	0.885
B2	9360	7960	−15.0	0.916	9206	−1.64	0.873
BR2	12400	11440	−7.76	0.801	12146	−2.05	0.787
SW2	12700	11780	−7.22	0.492	12373	−2.57	0.516

$$E_{x1},\ E_{y1}(E_{z1}),\ G_{yz1},\ G_{xy1}(G_{xz1}),$$
$$E_{x2},\ E_{y2}(E_{z2}),\ G_{yz2},\ G_{xy2}(G_{xz2})$$

The parameters E_{x1}, $E_{y1}(E_{z1})$, G_{yz1}, $G_{xy1}(G_{xz1})$ are elastic moduli of region 1 and E_{x2}, $E_{y2}(E_{z2})$, G_{yz2}, $G_{xy2}(G_{xz2})$ are those of region 2 as shown in Fig. 7. The Poisson's ratio is not considered as a design variable because it's influence is too small compared with any elastic modulus and it is a dependent variable of orthotropic material to confirm the stiffness matrix of the finite element to be a positive definite matrix (Peter Kohnke, 1994).

The natural frequencies of the VCM coil are chosen as modal parameters for the model updating process. To find the influence of the design variables on the natural frequencies of the VCM coil, structural sensitivity analysis is performed using the finite difference method. Fig. 8 shows the sensitivities of the design variables for eight natural frequencies. Before identification of the orthotropic material properties, the initial finite element model is assumed to have the isotropic material properties and the initial values of the elastic moduli and the Poisson's ratio are given as $E=30$ GPa, $G=10$ GPa, $\nu=0.3$.

As shown in Fig. 8, the sensitivities of E_{x1}, G_{xz1}, E_{y1} and E_{y2} for the natural frequencies are greater than another. The sensitivities of E_{x2}, G_{yz1}, G_{yz2} are so small that the natural frequencies of the VCM coil model are not much varied. To find the optimal values for the design variables that can reduce the error between the results of the EMA and the finite element analysis, an auto-model updating program is applied to the finite element model of the VCM coil. The result of the model updating is listed in Table 1 and the updated material properties of the VCM coil are presented in Table 2. Differences in natural frequencies between the predictions of the updated finite element model and the measured values are reduced from a maximum value of 35% to less than 5%. Optimal values of the orthotropic material properties are acquired from the result of the model updating and an equivalent finite element model of the VCM coil is constructed. The design variables of the orthotropic elastic moduli, are selected in ascending order and auto-model updating is performed with increase in the design variables.

Table 2 Orthotropic elastic modulus of equivalent VCM coil model

Design variable		Initial Values	Updated Values
E_{x1}	[GPa]	31.0	46.6
$E_{y1}(E_{z1})$	[GPa]	31.0	59.0
G_{yz1}	[GPa]	10.0	14.6
$G_{xz1}(G_{xy1})$	[GPa]	10.0	2.87
ν_{yz1}		0.3	0.3
$\nu_{xz1}(\nu_{xy1})$		0.3	0.3
E_{x2}	[GPa]	30.0	30.0
$E_{y2}(E_{z2})$	[GPa]	30.0	39.8
G_{yz2}	[GPa]	10.0	10.0
$G_{xz2}(G_{xy2})$	[GPa]	10.0	3.85
ν_{yz2}		0.3	0.3
$\nu_{xz2}(\nu_{xy2})$		0.3	0.3

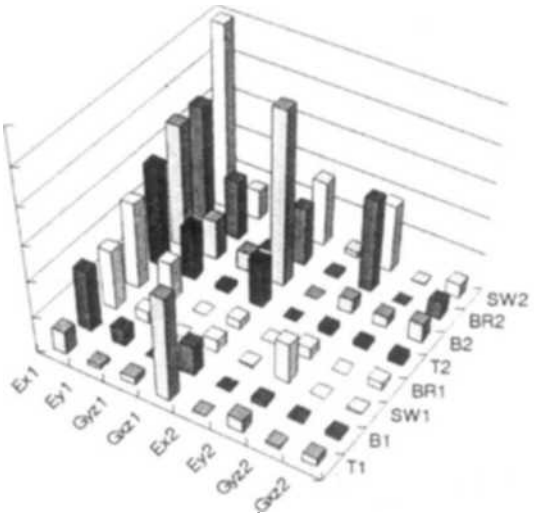

(a) 3 dimensional plot for sensitivity

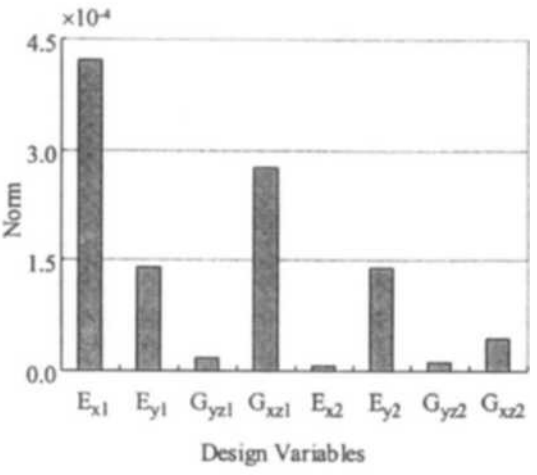

(b) Sensitivity norm of design variable

Fig. 8 Sensitivity of natural frequencies w.r.t. the orthotropic elastic modulus

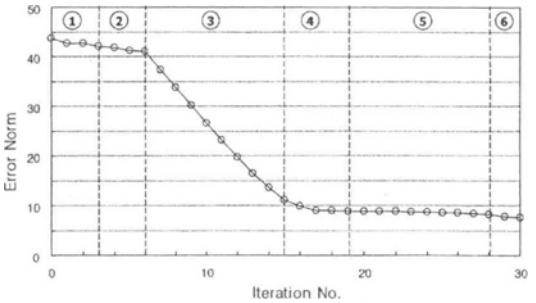

Fig. 9 Error norm of finite element model in model-updating process

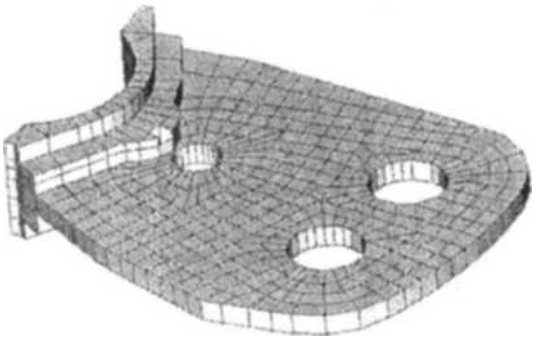

Fig. 10 Finite element model of the VCM part

Fig. 9 shows the decrease in the error norm during the iterative model updating process and the number in the circle denotes the number of design variables selected. When three design variables with large sensitivities (E_{x1}, G_{xz1}, E_{y1}) are selected, remarkable decrease in the error norm is noted. But two design variables with small sensitivities (E_{x2}, G_{yz2}) make no contribution during the model updating process.

3. Finite Element Modeling of the VCM Part

The holder part is made of the composite material. It is assumed to have an isotropic property and the material properties are referred to the data given by the manufacturer. (Kim et al., 1999) The finite element model of the VCM part is made up of 529 solid elements and 1121 nodes as shown in Fig. 10. The equivalent VCM coil model is merged into this model with estimated material properties. The FRF of the VCM part is measured at 12 measurement points in the vertical

Table 3 Natural frequencies of the VCM part

Mode #	EMA (Hz)	FEA (Hz)	Error (%)
1st Torsion mode	2330	2447	5.03
1st Bending mode	3330	3148	−5.46
1st Membrane Mode	5860	5804	−0.96
2nd Torsion mode	7600	7048	−7.26

direction by using the impact hammer and LDV. Measured and calculated natural frequencies are listed in Table 3. The finite element model of the VCM part also shows errors in the natural frequencies compared with the result of the EMA.

4. Finite Element Modeling of the E-block

The arm part of the E-block is made of an aluminum alloy and the material properties are referred to the data given by the manufacturer. (Kim et al., 1999) The finite element model of the arm part consists of 663 solid elements and 1521 nodes as shown in Fig. 11. The experimental modal analysis is performed to measure the modal parameters in the same manner as the test involving the VCM coil. An impulsive force is applied to the middle part of the E-block using a small impact hammer to transmit sufficient energy to the whole arm part ; 38 measurement points are selected to identify the mode shape of the E-block. The measured and calculated natural frequencies are listed in Table 4.

Table 4 Natural frequencies of the E-block

No	EMA [Hz]	EMA [Hz]	Error [%]	Mode shape
1	1760	1780	−1	1, 4 arm bending (out of phase)
2	2000	1970	2	1, 4 arm bending (in phase)
3	4560	4234	7	1, 2, 3, 4 arm bending
4	8320	8907	−7	1, 4 arm torsion (out of phase)
5	8610	9240	−7	1, 4 arm torsion (in phase)
6	10300	10804	−5	1, 4 arm torsion (out of phase)
7	10670	10987	−3	1, 4 arm torsion (in phase)

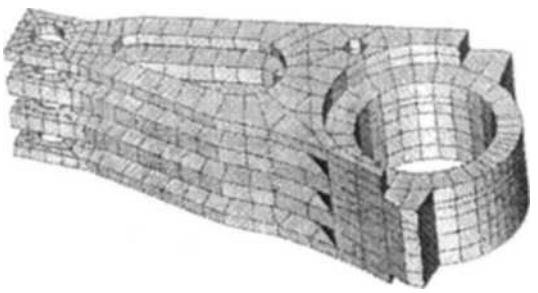

Fig. 11 finite element model of the E-Block

The modes with the bending mode shapes exist in the low frequency range while those with an arm torsion mode shape that can generate an off-track error of the slider head exist in the high frequency range. The majority of the mode shapes show deformation of the 1st and 4th arms because the thickness of the 2nd and 3rd arms is thicker than that of the 1st and 4th arms. The result shows a good agreement between the finite element model and the actual model.

5. Dynamic Characteristics of the HDD Actuator without a Suspension

The finite element model of the HDD actuator without a suspension is composed of the VCM part, E-block, pivot bearing finite element model. All sub-component finite element models are merged to construct the finite element model of the actuator assembly. It is made up of 1352 solid elements, 32 linear spring elements and 2820 nodes. The pivot bearing is modeled as a steel shaft and linear spring elements. The inner face of the shaft is constrained in all degrees of freedom to provide the fixed boundary condition. The free boundary condition is applied to the top of the shaft to coincide with the test condition without a cover.

The actual bearing part is made up of two ball bearings that are mounted on the E-block center hole. The span between the upper and lower bearings is 5.8 mm and each bearing has 13 balls. The bearing is modeled as 16 spring elements - 8 spring elements in the radial direction represent the radial stiffness of the bearing and 8 spring elements in the axial direction represent the axial stiffness of the bearing. One end of the axial spring is connected with the shaft and the other end is fixed. One end of the radial spring is connected with the shaft and the other end is connected with the E-block. The stiffness of springs is 600,000(mN/mm) in the radial direction and 450,000(mN/mm) in the axial direction. These values are initially obtained from the data given by the manufacturer and further tuned by applying the experimental results.

Table 5 Natural frequencies of HDD actuator without a suspension (FEA#1 : with un-tuned coil, FEA#2 : with tuned coil)

No	EMA (Hz)	FEA#1 (Hz)	Error (%)	FEA#2 (Hz)	Error (%)	Mode shape
1	611	683	−11.8	637	−4.19	VCM 1st bending
2	1340	1580	−17.9	1308	2.39	VCM 1st torsion
3	1540	1486	3.51	1483	3.70	1, 4 arm bending (in phase)
4	1820	1843	−1.26	1843	−1.26	1, 4 arm bending (out of phase)
5	2180	2154	1.19	2153	1.24	2, 3 arm bending (in phase)
6	2780	2720	2.16	2720	2.16	2, 3 arm bending (out of phase)
7	3340	3657	−9.49	3438	−2.93	VCM 2nd bending
8	3490	3559	−1.98	3525	−1.00	Lateral translation
9	3640	3968	−9.01	3879	−6.57	VCM 2nd torsion
10	–	3742	–	3710	–	Longitude translation
11	4990	4898	1.84	4704	5.73	E-block 1st bending
12	5620	6146	−9.36	5770	−2.67	VCM local bending
13	6100	7101	−16.41	6531	−7.07	VCM local torsion
14	7900	8634	−9.25	8284	−4.86	Lateral bending

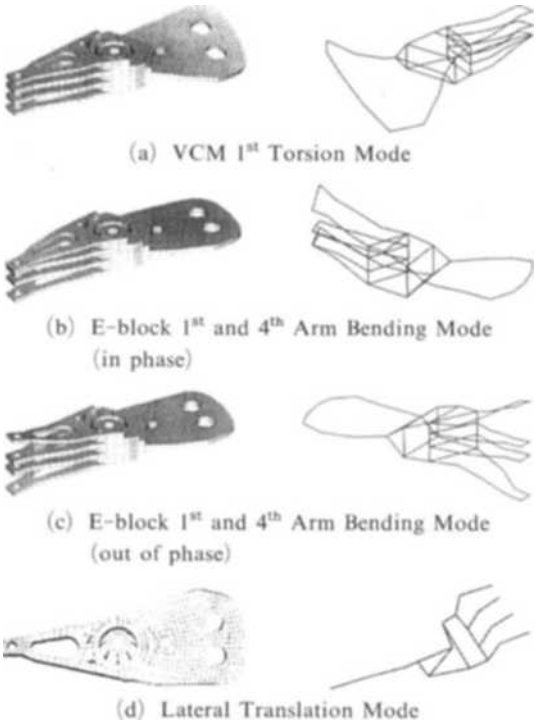

Fig. 12 Mode shapes of HDD actuator without a suspension

The number of the measurement points and locations are sum of those of the components. This actuator is assembled to a pivot mounted on a jig. The impact hammer is used to excite the specimen. The velocity responses are measured at the total of 57 points in the vertical direction by LDV. An additional modal testing is performed in the lateral direction to measure the lateral modes. Finally, the modal parameters are estimated using the Star-Modal software.

Table 5 shows the results of the finite element analysis and the EMA. Two finite element model are used to evaluate the effectiveness of the VCM coil model updating. FEA#1 show the result of the finite element analysis wity the VCM coil model that uses the initial values of the design variables geven in Table 2. FEA#2 shows the result of the finite element analysis with the VCM coil model using the updated values of the design variables listed in Table 2. There are several recent works reported about similar HDD actuator models Kim C. S. et al (1999) identified the dynamics characteristics of the HDD actuator system by using analytical and experimental modal analysis. In this work, the frequency difference between the experimental and FEA results are about 9% for vibration modes related to the

VCM part. Chang S. Y. et al (2000) performed a study about the topology optimization of the HDD actuator arm. In this work, the frequency difference between the experimentel and FEA results are over 20% for vibration modes related to the VCM part. These large errors for vibration modes in finite element model are caused by modeling inaccuracies of the VCM part.

In most vibration modes that are related to the VCM part, the differences in the natural frequencies between the experimental and FEA estimates are reduced in the updated model. The VCM 1st bending mode, the VCM 1st torsion mode, the VCM 2nd bending mode, the VCM 2nd torsion mode and the actuator lateral bending modes are improved through the model updating process. But the arm blade modes are not affected by model updating and dominated by the E-block part only.

Most natural frequencies calculated using the updated finite element model coincide with the results of the experimental modal analysis and the errors between them are less than 8%. It can be seen that the lateral translation mode (3532 Hz) and the longitudinal translation mode (4051 Hz) are strongly related to bearing stiffness. As shown in Fig. 13, the mode shape of the lateral translation and lateral bending modes show actuator movement in the lateral direction that can generate an off-track error because the head position is off from the centerline of the arm of E-block. The natural frequency of the lateral translation mode is lower than that of the lateral bending mode so that the lateral translation mode limits the bandwidth of the track following servo. To enhance the performance of the track following servo, this lateral translation mode must be raised.

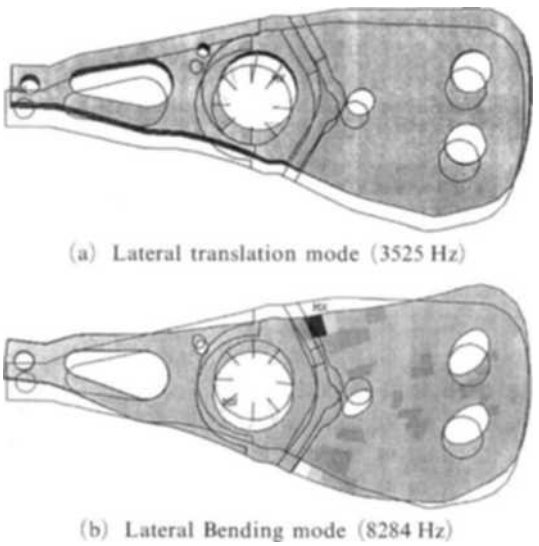

Fig. 13 Mode shapes of HDD actuator that limit the bandwidth of track following sevo

Because the thicknesses of the 2nd and 3rd arms are thicker than that of the 1st and 4th arms, the frequencies of the 1st-4th arm blade bending modes are lower than those of the 2nd-3rd arm blade bending modes. The result shows that the suspensions mounted on the 1st and 4th arm blades are susceptible to the vertical shock and vibration that generates the head slap motion. From the viewpoint of shock transmission, the 1st and 4th arm blade bending modes (both in-phase and out-of-phase directions) are main obstacles to reducing the shock transmission from the HDD case to the head mounted on the suspension.

6. Conclusion

In this paper, the dynamic characteristics of the HDD actuator system that are critical to improved servo performance and shock resistance are investigated using the finite element and experimental modal analyses methods. An equivalent finite element model of the VCM coil was constructed using the solid element that has a different elastic modulus for each direction to properly represent the anisotropy. Consequently, five local coordinates are introduced and elastic modulus sets for 2 regions are selected as design variables. To find the optimal values of the design variables, auto-model updating program is developed using MATLAB and CAE software ANSYS uses a sensitivity-based design parameter method and the physical parameters defined as the design variables are updated from the result of the previous sensitivity analysis. Improved strategy for selection of the design variables is developed to enhance the convergence rate. Structural sensitivities of the modal parameters with respect

to the design variables of the VCM coil are calculated and the error between the result of the finite element analysis and that of the EMA is found to be less than 5%.

A detailed finite element model of the sub-components of the HDD actuator is constructed using an auto-updating program. Using detailed sub-component models, the finite element model of the HDD actuator is constructed and vibration modes of the HDD actuator are investigated. The lateral translation mode of the HDD actuator without a suspension at 3.6 kHz can produce the residual vibration in settling operation and limit the servo bandwidth. The 1st and 4th arm blade bending modes (both in-phase and out-of-phase directions) are found to be the main obstacles to reducing the shock transmission from the HDD case to the head mounted on the suspension.

Acknowledgment

This research has been supported by KOSEF (Grant No. 2000G0102) and the authors are grateful for the support.

References

Chang, S. Y., Youn, S. K., Kim, C. S. and Oh, D. H. 2000, "Topology Optimization of a HDD Actuator Arm," Transactions of KSME(A), Vol. 24, No. 7, pp. 1801~1809, in Korean.

Chiou, S. S., Miu, D. K., 1992, "Tracking Dynamics of In-line Suspensions in High-Performance Rigid Disk Drives with Rotary Actuators," J. of Vibration and Acoustics 114, pp. 67~73.

Heath, J., 2000, "Simple Approach to Improved Actuator Bandwidth," Data Storage, September, pp. 48~60.

Heylen, W., Lammens, S., Sas, P., 1997, "Modal Analysis Theory and Testing," KU Leuven, A6.11~A6.15.

Jiang, L., Miles, R. N., 1999, "A Passive Damper for the Vibration Modes of the Head Actuator in Hard Disk Drive," J. of Sound and Vibration 220, pp. 683~694.

Kim, C. J., Chun, J. I., Byun, Y. K., Ro, K. C., Chyng, C. C. and Jeong, T. G., 1997, "Suspension Dynamics of HDD for High Track Density," Transactions of KSME(A), Vol. 21, No. 11, pp. 1885~1895, in Korean.

Kim, C. S., Chun, C. J. and Ro, K. C. 1999, "Modal Analysis of Hard Disk Drive Actuator," Proceedings of the KSNVE, Spring Annual Meeting, pp. 129~133, in Korean.

Kim, D. W. and Park, Y. P., 2000, "Modal Tuning of HDD Suspension System," Proceedings of the KSNVE 2, Spring Annual Meeting, pp. 1583~1588.

Kohnke, P., 1994, "ANSYS Theory Reference Release 5.6," 11th edition, SAS IP, Inc., pp. 2-3~2-8

Lee, J. Y., 2002, "A Structural Eigenderivative Analysis by Modification of Design Parameter," Transactions of KSME(A), Vol. 26, No. 4, pp. 739~744, in Korean.

Marek, S., Carlson, P. and Resh, R., 1995, "Why Head Suspension need Shock Treatment," Data storge, Volume 2, Issue 7.

Miu, D. K. and Karam, R. M., 1991, "Dynamic and Design of Read/Write Head Suspensions for High Performance Rigid Disk Drives," Advanced Information Storage System 1, pp. 145~153.

Ohwe, T., Watanabe, T., Uoneoka S. and Mizoshita, Y., 1996, "A New Integrated Suspension for Pico-Sliders (Pico-Caps)," IEEE Transactions on Magnetics 32, Vol. 5, pp. 3648~3650.

Ohwe, T., Yoneoka, S., Aruga, K., Yamada, T. and Mizoshita, Y., 1990, "A Design of High Performance Inline Head Assembly for High-Speed Access," IEEE Transactions on Magnetics 26, Vol. 5, pp. 2445~2447.

Sohn, K., Okuma, M. and Nagamatsu, A., 1992, "Correction of Finite-Element Models using Experimental Modal Data (Consideration of Sensitivity with respect to Material Constants)," JSME (C) 58, pp. 2962~2969, in Japanese.

Sohn, J. S., Choa, S. H., Lee, H. S. and Hong, M. P., 2001, "Analysis of Shock Mechanism and Actuator Behavior of HDD," Journal of KSNVE, Vol. 11, No. 3, pp. 449~454, in Korean.

Sun, L. Y., Yu, C. S., Zhang, B. J., Chen, N. and Sun, Q. H., 2000, "Finite Element Model Updating Via Automatic Optimization of Physical Parameters," IMAC, pp. 1544~1548.